

See discussions, stats, and author profiles for this publication at: <https://www.researchgate.net/publication/367441749>

# Optimal design and operation of solar energy system with heat storage for agricultural greenhouse heating

Article in Energy Conversion and Management X · April 2023

DOI: 10.1016/j.ecmx.2023.100353

---

CITATIONS

0

READS

190

2 authors, including:



Parastoo Mohebi

Sharif University of Technology

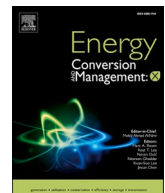
1 PUBLICATION 0 CITATIONS

[SEE PROFILE](#)

Some of the authors of this publication are also working on these related projects:



Thermoeconomic analysis of solar collectors and heat storages [View project](#)



# Optimal design and operation of solar energy system with heat storage for agricultural greenhouse heating

Parastoo Mohebi, Ramin Roshandel\*

*Department of Energy Engineering, Sharif University of Technology, Tehran, Iran*



## ARTICLE INFO

**Keywords:**

Design and operation optimization  
Heat storage  
Solar thermal collector  
Agricultural greenhouse

## ABSTRACT

A significant challenge of agricultural greenhouses is their high energy demand which is mainly satisfied by fossil fuels resulting in climate change impacts. In this paper, a joint design-operation linear optimization framework for a solar energy system with heat storage is developed to fulfill the agricultural greenhouse heating load. The energy system consists of solar collector, backup boiler, and short-long term heat storages. The developed framework is applied to reach minimum-cost solution. Then, the effects of emission reduction policies, greenhouse cultivation scheduling, natural gas price, and investment cost scenarios are investigated. Furthermore, a multi-objective optimization is performed in terms of minimizing CO<sub>2</sub> emissions and total annual cost using epsilon-constraint method. The optimal energy system due to the minimum-cost solution includes a 1065 m<sup>2</sup> solar collector and a 1265 kW boiler in combination with 967 kWh and 25 MWh short-term and long-term heat storages, respectively. The 30 % carbon reduction policy results in a 70.5 % increase in solar collector area. The selected optimal solution of the Pareto front, which is the closest solution to the ideal point, has 35.3 % more annual cost and 89.5 % less CO<sub>2</sub> emissions compared to the minimum-cost solution.

## 1. Introduction

Ensuring availability of clean energy, food, and clean water are three of seventeen goals of the 2030 UN sustainable development [1]. The population of the world is expected to be 8.5 billion by 2030. Population growth, along with dietary change, urbanization, and other consequences of economic growth, lead to a considerable increase in energy, water, and food demand. This increasing demand puts pressure on supply resources and can cause a resource shortage [2–4]. Agricultural greenhouses are the junction of energy-food-water nexus by raising the production yield as well as reducing water demand. However, their energy requirement can be a hundred times more than conventional cultivation [4,5]. Thus, energy consumption is a significant challenge in expansion of greenhouses [6], while most of the required energy in cold and even moderate climates is due to heating [7–9].

Greenhouses conventionally rely on carbon-based fuels, contributing to climate change impacts, high production costs, and growing concerns over fossil fuel depletion [8,10–14]. These issues necessitate the utilization of renewable energy resources [13,14]. From the environmental and sustainable point of view, solar energy is a clean, renewable, and necessary component of the sustainable energy future in agriculture,

including greenhouse applications [4,15,16]. However, solar energy is an intermittent energy source. The highest solar energy production occurs in summer, while the highest heating demand is required in winter [17,18]. Seasonal thermal energy storage is a promising solution to store summer heat for winter use [19,20]. Thus, the mismatch between the greenhouse heating demand and the availability of solar thermal energy can be compensated by using heat storage systems [13].

Numerous articles described and evaluated the ability of different thermal energy storage systems to overcome the mismatch between energy supply and demand [21–23]. Esen et al. [22] conducted a parametric study to determine the time dependency of the stored energy in a tank containing phase change materials. In addition, a theoretical model was developed to predict the effects of various thermal and geometric parameters on the melting time for different phase change materials and tank configurations [23].

In particular, a number of studies have been conducted to assess the performance of a solar energy system combined with seasonal heat storage for the purpose of heating greenhouses [8,16,24–26]. The potential of implementing large-scale solar collector system in combination with seasonal heat storage for greenhouse applications is investigated by Semple et al. [8]. This study simulates the borehole thermal energy storage system using TRNSYS software. The investigated

\* Corresponding author.

E-mail address: [roshandel@sharif.edu](mailto:roshandel@sharif.edu) (R. Roshandel).

Nomenclature	
Abbreviations	
LP	linear programming
LTS	long-term heat storage
MILP	mixed-integer linear programming
SCO	solar thermal collector
SOC	state of charge
STS	short-term heat storage
Chemical formulas	
CO <sub>2</sub>	carbon dioxide
Variables and parameters	
A	area [m <sup>2</sup> ]
b <sub>1</sub>	first-order heat loss coefficient [W/Km <sup>2</sup> ]
b <sub>2</sub>	second-order heat loss coefficient [W/K <sup>2</sup> m <sup>2</sup> ]
C	specific heat [J/kg·K]
C <sub>fuel</sub>	fuel annual cost [Euro]
C <sub>investment</sub>	investment annual cost [Euro]
C <sub>O &amp; M</sub>	operation and maintenance annual cost [Euro]
Cap	technology capacity [kW]
CRF	capital recovery factor
E	stored energy [kWh]
e	specific emission [kg CO <sub>2</sub> /kWh]
f	objective function
G	solar irradiation [W]
H	length of a side of the pitched roof of greenhouse [m]
h	height of greenhouse [m]
L	length of greenhouse [m]
Loss	heat loss [kW]
N	infiltration rate [s <sup>-1</sup> ]
n	system lifetime [year]
P	charge and discharge power of heat storage [kW]
Q	thermal power [kW]
Size	storage size [kWh]
T	temperature [°C]
U	overall heat transfer coefficient [W/m <sup>2</sup> K]
u	fuel price [EUR/kWh]
V	volume [m <sup>3</sup> ]
y	discount rate [%]
Superscripts	
max	maximum
Min	minimum
T	length of the time horizon [hour of the year]
t	time step [hour of the year]
Subscripts	
a	ambient
air	air
ch	charge
dch	discharge
g	greenhouse
i	technology index
in	index of input power
j	objective function index
m	number of Pareto solutions
NG	natural gas
n	total number of objective functions
o	optical
p	panel
Greek letters	
γ	cost coefficient [%]
η	efficiency [%]
θ	roof pitch angle [°]
Λ	loss coefficient of heat storage [h <sup>-1</sup> ]
μ	cost coefficient
ξ	fraction of incident light absorbed by the canopy [%]
ρ	density [kg/m <sup>3</sup> ]
φ	ventilation rate [m <sup>3</sup> /s]

energy system can reduce annual CO<sub>2</sub> equivalent emissions by about 220 tonnes per acre. Zhang et al. [16] constructed and investigated a seasonal solar heat storage system that provides greenhouse heating demand. The system proved that seasonal thermal energy storage is a feasible technology that can partially solve the heat load and solar energy mismatch between summer and winter months.

A significant challenge of implementing solar collectors and thermal energy storage is their high required investment costs. The financial and environmental advantages of energy storage can be guaranteed and increased further by optimization of the design and operation of the overall energy system [27,28]. There are various approaches to handle the optimization procedure. The most commonly applied methods are linear programming (LP) [29–31], mixed-integer linear programming (MILP) [28,32–34], and heuristic methods (genetic algorithms and particle swarm optimization) [27,35–37].

Various researchers optimized energy systems, including solar collectors in combination with heat storage. Studies considering single-objective optimization mainly aim to minimize total cost [38,39]. Durao et al. [36] developed a framework based on Matlab/Simulink, which can simulate and optimize the sizing of a greenhouse solar heating system equipped with long-term heat storage. In this study, the genetic algorithm was employed as the optimization algorithm, and a constant rate of 50 kW was considered for heating load in the winter.

In order to generalize the outcomes for decision-making, multi-objective optimization is required [40]. Multi-objective optimization can show the trade-offs between conflicting objectives [41]. Different approaches could be implemented to achieve a whole Pareto front, such as the epsilon constraint method [29,32,33] and weighted sum method

[42]. Dorotić et al. [29] developed a multi-objective optimization for district heating, minimizing economic, ecological, and exergy destruction objective functions. This LP model optimizes the design and hourly operation of the energy system. Gabrielli et al. [32] developed a multi-objective MILP methodology to optimize the design and operation of a multi-energy system, in terms of minimizing total cost and CO<sub>2</sub> emissions objective functions.

Regarding the literature review, there is a lack of hourly-based operation optimization for a solar energy system, including long-term heat storage, to cover greenhouse energy demand. Hourly operation of this energy system for a whole year is essential since the greenhouse heating load has a significant seasonal effect. Secondly, design/operation optimizations of such energy systems are carried out using nonlinear techniques, which can not guarantee the global optimality of results. Lastly, previous studies have not evaluated the impact of the dynamic greenhouse heating demand on the optimal energy system under different growing seasons.

The current paper presents an optimization framework for a hybrid solar energy system with long-term heat storage that satisfies the heating demand of a greenhouse while minimizing total annual cost. This developed framework optimizes sizing and hourly-based operation of the energy system for the time horizon of a whole year to take seasonal characteristics into account. The global optimal solution is achieved using Cplex solver. The energy system under investigation consists of short-term and long-term heat storage systems, solar thermal collectors, and a backup boiler. Additionally, this research evaluates the impacts of carbon reduction policies, greenhouse cultivation scheduling, natural gas price, and solar collector investment cost scenarios on the optimal

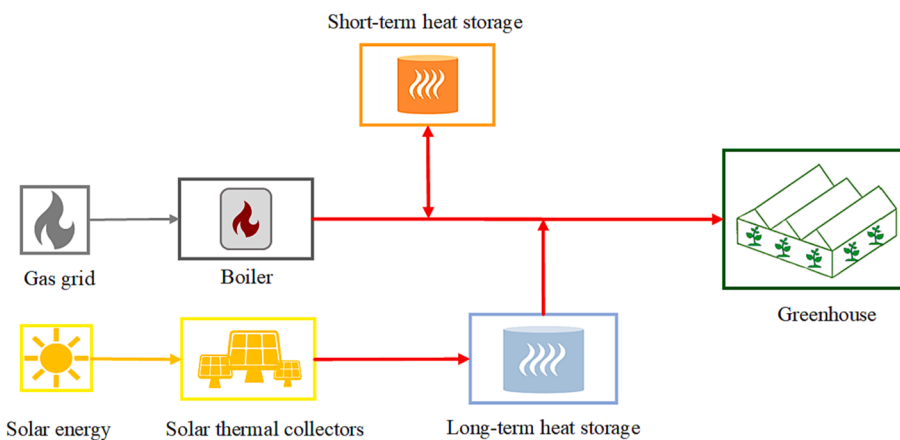


Fig. 1. Schematic representation of the investigated energy system.

design and operation of the investigated system configuration. Ultimately, the epsilon-constraint method is applied for multi-objective optimization to minimize CO<sub>2</sub> emissions along with the total annual cost. The optimal design and energy flows associated with the closest solution to the ideal point are determined using the LINMAP decision-making approach.

The proposed method is novel since, to the best of our knowledge, no previous study has presented a linear methodology for optimizing the joint design and hourly operation of a solar energy system with long-term heat storage that meets the hourly heating demand of a greenhouse for an entire year. Additionally, no prior research has investigated the effect of greenhouse heating demand under various cultivation scheduling scenarios (different growing seasons) on the optimal design and operation of the energy system.

In summary, the main objective of the study is to decarbonize agricultural greenhouses through the use of solar energy to supply heating demand, while long-term heat storage is implemented to compensate for the mismatch between heating load and solar thermal energy availability. The developed framework optimizes decarbonization-cost trade-offs. The scientific contributions of the current paper are as follows:

- Development of LP model for a hybrid solar energy system, including heat storage that minimizes total annual cost. This model guarantees the global optimal solution.
- Presentation of multi-objective optimization framework, which can show the trade-offs between conflicting objectives, including total annual cost and CO<sub>2</sub> emissions, using epsilon-constraint and LINMAP methodologies.
- Development of joint design and operation optimization considering hourly energy flows as operation decision variables in addition to solar collector area, boiler, and heat storage capacities as design decision variables.
- Integrated assessment of the carbon reduction policies, greenhouse cultivation scheduling, natural gas price, and investment cost scenarios on optimal design and energy flows.

This article is organized as follows: Section 2 provides an overview of the studied energy system, input data, and mathematical formulation of the optimization framework. Section 3 describes the case study region, and Section 4 offers the acquired results and discussions. Finally, the conclusions and future work ideas are presented in Section 5.

## 2. System description and methodology

The considered hybrid energy system of this study has the primary objective of providing heating demand of a greenhouse. As shown in Fig. 1, the energy system under investigation involves short-term and

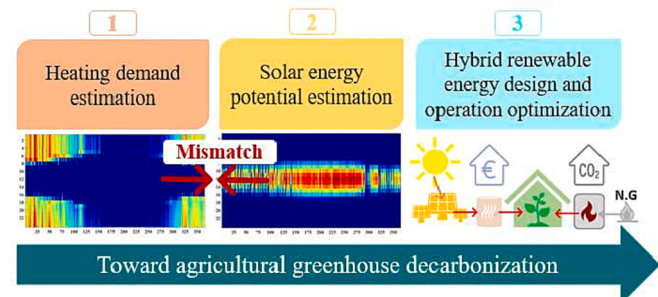


Fig. 2. Overall methodology of the current research.

long-term heat storage systems, solar thermal collectors, and a backup boiler. Short-term heat storage acts as a buffer for the system, while long-term heat storage is charged by solar thermal collectors and is used as seasonal storage.

The overall methodology of the current research is depicted in Fig. 2. The first stage of decarbonization of greenhouse is to (1) analyze the greenhouse heating demand; for this, a climate-based energy demand model is utilized. Then (2) solar potential availability is determined using historical data of solar insolation in the case study region, and finally (3) the proposed hybrid renewable energy system is optimized by developing an optimization framework. The outcomes of this framework are the optimal design of hybrid renewable energy (optimal sizing of solar collector, natural gas boiler, and storage system) in addition to optimal energy flows in the proposed system.

Fig. 3 presents the overview of the optimization framework, which returns optimal sizing and hourly energy flows of the system for a whole year considering objective function of minimizing total annual cost. The total cost includes the investment cost of the solar collector, natural gas boiler, and heat storage system, in addition to operation cost, including natural gas and maintenance costs.

The input data of the framework includes hourly profiles of weather conditions, greenhouse heating demand, and specific solar collector heat production, as well as techno-economic information. The following is a detailed explanation of the optimization framework in terms of input data, decision variables, constraints, objective functions, and implemented approach for multi-objective optimization.

### 2.1. Input data

The input data of the optimization framework are assumed to be constant throughout the lifetime of the system. The greenhouse heating demand and solar collector heat production models are presented in this

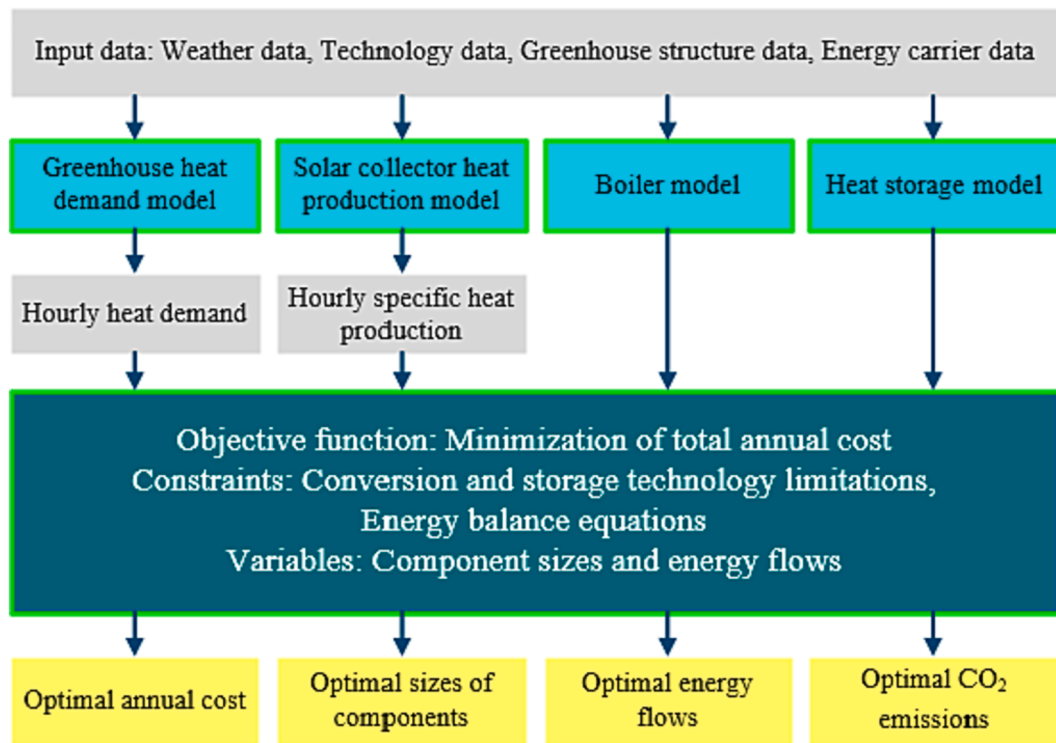


Fig. 3. Overview of the optimization framework.

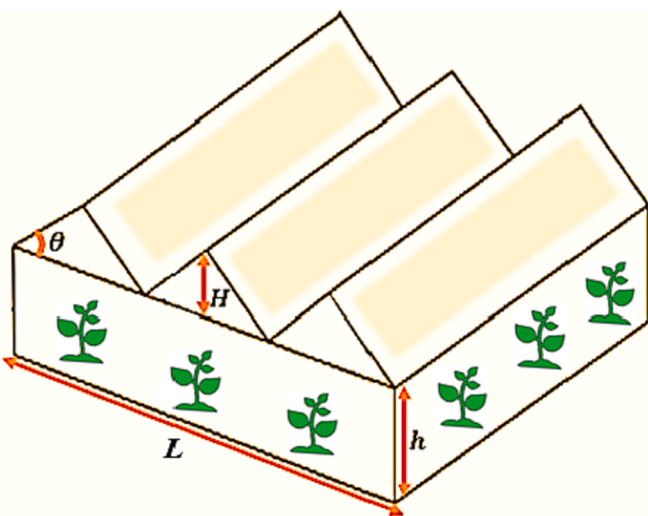


Fig. 4. Representation of a Venlo-type greenhouse.

**Table 1**  
Input data of the greenhouse heating demand model.

Parameter	Unit	Value	Reference
$N$	$\frac{1}{s}$	$2.1 \times 10^{-4}$	[47,48]
$U$	$\frac{W}{m^2 K}$	4	[47,48]
$h$	m	4	[47]
$\theta$	°	30	[47]
$H$	m	2	[47]
$L$	m	100	Assumption
$T_a$	°C	Hourly distributed	[43]
$T_g$	°C	19 (day)- 16 (night)	[4]
$G$	W	Hourly distributed	[43]

section since their hourly outputs are used in the optimization model as input parameters. In short, the inputs to the developed framework are:

- The hourly weather conditions, including air temperature and solar radiation, obtained from publicly available resources [43].
- Physical characteristics of greenhouse structure.
- The technical and economic parameters of solar thermal collector, short-term and long-term heat storages, and backup boiler.
- The price and emission coefficient of fossil fuel carrier used in the hybrid energy system.
- The hourly heat demand profile of the greenhouse for a whole year, which is output of the heating demand model presented in section 2.1.1.
- The hourly heat production profile of the solar collector, which is output of the solar collector model presented in section 2.1.2.

### 2.1.1. Greenhouse heating demand

Several researchers have developed approaches to determine greenhouse energy demand [7,44–46]. In this study, the heating demand of greenhouse is calculated by the model presented in [10,47]. This model is based on energy balance and considers three mechanisms: energy transfer between indoor and outdoor conditions, heat transfer due to ventilation, and energy transfer related to solar radiation. Therefore, the energy demand of greenhouse is calculated with Eq. (1):

$$Q_g = A_g U (T_g - T_a) + C_{air} \varphi \rho_{air} (T_g - T_a) - \xi G \quad (1)$$

Where  $A_g$  is the total area of the cover,  $U$  is the overall heat transfer coefficient of the greenhouse structure,  $C_{air}$  is the specific heat of the air,  $\varphi$  is the ventilation rate,  $\rho_{air}$  is the density of the air,  $\xi$  is the fraction of the incident light due to absorptivity of the canopy,  $G$  is the total solar irradiation, and  $T_a$  is the ambient air temperature.  $T_g$  is the greenhouse interior air temperature considered to be the minimum suitable temperature for 100 % possible growth of crops like tomato, pepper, and eggplant [4].

By considering Venlo greenhouse structure similar to Fig. 4 and also

ASABE [48] simplifications for energy demand, Eq. (1) can be approximated by:

$$Q_g = (4Lh + \frac{L^2}{\cos\theta})U(T_g - T_a) + 1800(h + \frac{H}{2})L^2N(T_g - T_a) - \xi G \quad (2)$$

Where  $L$  is the greenhouse length/width considering a square footprint based on [47],  $N$  is the infiltration rate,  $h$  is the greenhouse height,  $\theta$  is the roof pitch angle, and  $H$  represents the length of a side of the pitched roof. The values of input parameters for greenhouse energy model are presented in Table 1.

Eq. (2) is improved to determine the heating demand at time step t:

$$\begin{aligned} Q_g^t &= \left(4Lh + \frac{L^2}{\cos\theta}\right)U(T_g - T_a^t) + 1800\left(h + \frac{H}{2}\right)L^2N(T_g - T_a^t) - \xi G^t \\ &= 1, 2, \dots, 8760 \end{aligned} \quad (3)$$

Active cooling is required whenever the heating load becomes negative, according to Eq. (3).

### 2.1.2. Specific collector heat production

A flat plate collector model is used to calculate solar thermal collector (SCO) heat production according to [49]. The specific thermal output of SCO at time step t is formulated as follows:

$$Q_{Specific,SCO}^t = \eta_o G_{SCO}^t - b_1(T_p - T_a^t) - b_2(T_p - T_a^t)^2 \quad (4)$$

Where  $Q_{Specific,SCO}^t$  represents collector heat production and  $G_{SCO}^t$  is specific solar irradiation, assuming a south-oriented collector, tilted 35° with respect to horizontal plane, and no shading effect.  $T_p$  and  $T_a^t$  are the mean panel temperature and ambient temperature, respectively.  $G_{SCO}^t$  and  $T_a^t$  are obtained from publicly available databases [43].  $\eta_o$  is known as optical efficiency.  $b_1$  and  $b_2$  represent temperature dependent coefficients. In this research, these parameters are assumed, corresponding to an Arcon Sunmark HT-SolarBoost 35/10 flat plate collector [49]. When the heat output becomes negative based on Eq. (4), it is set to be 0 W [27,29,34,50].

## 2.2. Decision variables

The optimization decision variables are as follows:

- Design variables, including:
  1. Short-term and long-term heat storage sizes ( $Size_{sts}$  and  $Size_{lts}$ )
  2. Solar collector area ( $A_{SCO}$ )
  3. The capacity of the boiler ( $Cap_{boiler}$ )
- Operation variables are determined at every hour of the year, including:
  1. Natural gas consumed in boiler in each hour
  2. The hourly input and/or output heat flows of solar thermal collector, boiler, and storage technologies
  3. The hourly stored energy in short-term and long-term heat storages

## 2.3. Optimization constraints

Optimization constraints can be classified into two categories. The first category includes constraints related to the performance of conversion and storage technologies, while the second category includes energy balance equations.

### 2.3.1. Solar collector

The solar collector output is obtained by Eq. (5):

$$Q_{SCO}^t = A_{SCO} Q_{Specific,SCO}^t \quad (5)$$

Where  $A_{SCO}$  represents the collector surface area, the only optimization variable related to the solar collector.

### 2.3.2. Short-term heat storage

The short-term storage is modeled through the following set of linear equations:

$$E_{sts}^t = E_{sts}^{t-1} + (\eta_{ch} P_{sts,ch}^t - \frac{P_{sts,dch}^t}{\eta_{dch}}) \Delta t - Loss_{sts}^t \Delta t \quad (6)$$

$$0 \leq E_{sts}^t \leq Size_{sts} \quad (7)$$

$$E_{sts}^{t=0} = E_{sts}^{t=T} \quad (8)$$

$$Loss_{sts}^t = \Lambda_{sts}^{storage} E_{sts}^{t-1} + \Lambda_{sts}^{static} Size_{sts} g(T_a^t) \quad (9)$$

$$g(T_a^t) = \frac{T_{max} - T_a^t}{T_{max} - T_{min}} \quad (10)$$

$$0 \leq P_{sts,ch}^t \leq Size_{sts} \quad (11)$$

$$0 \leq P_{sts,dch}^t \leq Size_{sts} \quad (12)$$

$E_{sts}^t$  is the actual level of energy stored at hour t and  $Size_{sts}$  is the capacity of heat storage. Eq. (6) states that the energy stored in each time step equals the energy stored in the former time step, increased by charged energy ( $P_{sts,ch}^t$ ) and reduced by energy output, resulted by either discharging ( $P_{sts,dch}^t$ ) or heat losses ( $Loss_{sts}^t$ ).  $\Delta t$  is the time interval duration (one hour). According to Eq. (7), the storage level is limited by the storage capacity. Eq. (8) guarantees an identical storage level in the last hour as in the first hour of the year. Heat loss of STS is described by considering the influence of ambient temperature through  $g(T_a^t)$ .  $\Lambda_{sts}^{storage}$  and  $\Lambda_{sts}^{static}$  in Eq. (9) are heat loss coefficients. The heat flows from/to heat storage are restricted by a maximum rate, which is a fraction of the storage capacity. As shown in Eq. (11) and Eq. (12), in this research, it is assumed that the maximum (dis)charge rate is the storage capacity [29,31,32,51].

### 2.3.3. Long-term heat storage

Long-term heat storage is modeled similarly to short-term heat storage with Eqs. (13)–(18), widely applied in modeling heat storages in LP optimization of energy systems [28,29,32,38]. It is considered that, unlike short-term storage, long-term storage is buried underground, which leads to ignoring the impact of ambient temperature.  $\Lambda_{lts}^{storage}$  represents the self-discharge parameter.

$$E_{lts}^t = E_{lts}^{t-1} + (\eta_{ch} P_{lts,ch}^t - \frac{P_{lts,dch}^t}{\eta_{dch}}) \Delta t - Loss_{lts}^t \Delta t \quad (13)$$

$$0 \leq E_{lts}^t \leq Size_{lts} \quad (14)$$

$$E_{lts}^{t=0} = E_{lts}^{t=T} \quad (15)$$

$$Loss_{lts}^t = \Lambda_{lts}^{storage} E_{lts}^{t-1} \quad (16)$$

$$0 \leq P_{lts,ch}^t \leq Size_{lts} \quad (17)$$

$$0 \leq P_{lts,dch}^t \leq Size_{lts} \quad (18)$$

### 2.3.4. Boiler

The boiler generates heat from natural gas and is expressed through Eq. (19) and Eq. (20) [32,52]. Ramping limits and size dependency of performance are neglected for simplicity.

$$Q_{boiler}^t = \eta_{boiler}^t Q_{boiler,in}^t \quad (19)$$

$$0 \leq Q_{boiler,in}^t \leq Cap_{boiler} \quad (20)$$

### 2.3.5. Energy balance equations

Eq. (21) and (22) formulate the energy balance between supply and

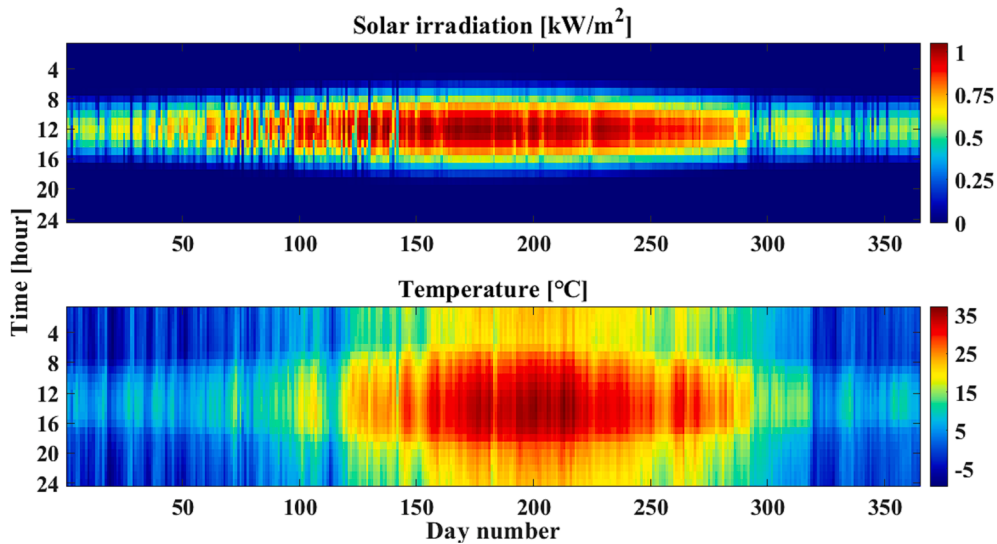


Fig. 5. Hourly solar irradiation and temperature for the case study region in 2019.

demand. Eq. (21) states that the greenhouse heating demand must be satisfied for every hour of the year by discharged energy from short-term and long-term heat storage systems and produced heat from the backup boiler while short-term storage can be charged.

$$Q_g^t = Q_{boiler}^t + P_{sts,dch}^t - P_{sts,ch}^t + P_{lts,dch}^t \quad (21)$$

$$P_{lts,ch}^t = Q_{sco}^t \quad (22)$$

#### 2.4. Objective functions

The developed multi-objective optimization framework is defined with two contrasting objective functions: (1) the total annualized cost and (2) the yearly CO<sub>2</sub> emissions of the system. The total annualized cost, ( $F_{annual\_cost}$ ), consists of three contributions, namely, investment cost ( $C_{investment}$ ), fuel cost ( $C_{fuel}$ ) and maintenance cost ( $C_{O\&M}$ ). Notably, the current ecological approach does not consider life cycle assessment and focuses on annual CO<sub>2</sub> emissions caused by natural gas consumption in the boiler. The objective functions are expressed as follows:

$$F_{annual\_Cost} = \sum_i C_{investment,i} + \sum_i C_{O\&M,i} + C_{fuel} \quad (23)$$

$$C_{investment,i} = \mu_i \cdot Cap_i \cdot CRF \quad (24)$$

$$C_{O\&M,i} = \gamma_i \cdot C_{investment,i} \quad (25)$$

$$C_{fuel} = \sum_{t=1}^T u_{NG} \cdot Q_{boiler,in}^t \quad (26)$$

$$CRF = \frac{y(1+y)^n}{(1+y)^n - 1} \quad (27)$$

$$F_{emission} = \sum_{t=1}^T e_{CO_2} \cdot Q_{boiler,in}^t \quad (28)$$

Where  $\mu_i$  is the cost coefficient and  $Cap_i$  is the size of the i-th technology. The annual investment cost is calculated using the capital recovery factor (CRF) [53].  $y$  and  $n$  indicate the discount rate and project lifetime assumed to be 5 % and 20 years, respectively. In addition, a constant natural gas price ( $u_{NG}$ ) of 0.03  $\frac{\text{Euro}}{\text{kWh}}$  is used [54,55]. The annual maintenance cost of each technology is a fraction ( $\gamma$ ) of its annual investment cost [32]. The specific carbon dioxide emission of natural gas ( $e_{CO_2}$ ), is assumed to be 0.22  $\frac{\text{kg CO}_2}{\text{kWh}}$  [56].

#### 2.5. Multi-objective optimization approach

In this paper, the epsilon constraint method is implemented for multi-objective optimization. This method translates the problem to a single objective optimization problem and considers other objectives as constraints, as shown in Eq. (29) and (30). In order to apply this method, the range of each objective function has to be recognized to ensure that assigned epsilon constraints are eligible. The typical approach is to calculate these ranges by individually optimizing the objective functions [29,32]. In this research, first, the total annual cost and annual emission of the system are optimized separately to achieve the upper and lower limits of each objective function. Then the emission interval is divided into equal steps, and the total annual cost is minimized while considering a maximum threshold for annual CO<sub>2</sub> emissions.

$$\min F_{annual\_Cost} \quad (29)$$

$$F_{emission} \leq \epsilon \quad (30)$$

#### 2.6. Decision-making approach

After implementation of multi-objective optimization, a decision-making process is required to select the final solution from the available optimal solutions of the Pareto front. Some researchers propose LINMAP method, which selects the solution with the least distance to the ideal point, as represented in Eq. (31) and (32) [57]. The ideal point is an infeasible solution where each objective is optimized, regardless of satisfaction with other objectives [29].

$$\min(d_m) \quad (31)$$

$$d_m = \sqrt{\sum_{j=1}^n (F_{mj} - F_j^{ideal})^2} \quad (32)$$

Where  $d_m$  is the distance to the ideal point, while  $m$  stands for each solution on the Pareto front, and  $n$  denotes the number of objectives. In Eq. (32),  $F_j^{ideal}$  is the ideal value for j-th normalized objective function and  $F_{mj}$  is the non-minimum value of the normalized objective function j.

### 3. Case study

The developed methodology is applied to meet the heating demand of a one-hectare greenhouse in Tehran, Iran considering meteorological profiles for 2019 [43]. Fig. 5 depicts the meteorological data, including air temperature and solar radiation. The maximum and minimum

**Table 2**  
Technology data.

	Parameter	Unit	Value	Reference
SCO (Solar thermal collector)	$\eta_o$	–	0.839	[49]
	$b_1$	$W$	2.46	[49]
	$b_2$	$Km^2$		
	$\mu$	$K^2m^2$	0.0197	[49]
STS (Short-term heat storage)	$\gamma$	$Euro$	190	[54]
	$\eta_{ch,dch}$	$m^2$		
	$\Lambda_{storage}$	%	3	[32]
	$\Lambda_{static}$	%	90	[51]
	$T^{min}$	%	0.06	[51]
	$T^{max}$	°C	0.053	[51]
LTS (Long-term heat storage)	$T^{min}$	°C	65	[32,51]
	$T^{max}$	°C	90	[32,51]
	$\mu$	$Euro$	4.5	[54]
	$\eta_{ch,dch}$	$kWh$		
Boiler	$\Lambda_{storage}$	%	99	[38]
	$\mu$	$day$	0.05	[54]
	$\eta_{boiler}$	$Euro$	0.9	[54]
$\mu$		$kWh$		
	$\gamma$	%	89	[54]
$\mu$		$Euro$	60	[54]
	$\gamma$	%	2	[32]

outside air temperatures are 37.3°C and –9.8°C, respectively [43]. The total and average solar radiation are approximately 2063  $\frac{kW}{m^2 \cdot year}$  and 235.5  $\frac{W}{m^2 \cdot hour}$ , respectively [43], making this location suitable for integrating solar thermal collectors. The technology-related parameters used in the optimization framework, along with their references, are listed in Table 2.

#### 4. Results and discussion

The results acquired in this paper are represented through six sections. Section 4.1 describes the outputs of the greenhouse heating demand and solar collector heat production models. Section 4.2 represents the significance of considering operation by comparing joint design-operation optimization with design optimization results in the minimum-cost solution. In section 4.3, a sensitivity analysis is conducted by changing heating demand. The obtained results of the base minimum-cost solution are shifted due to the implementation of CO<sub>2</sub> mitigation policies in section 4.4. Section 4.5 shows the impact of considering greenhouse cultivation scheduling on optimization results.

Section 4.6 investigates the effect of natural gas price and solar collector investment cost on optimal results. In Section 4.7, a two-dimensional Pareto front, the characteristics of the selected optimal solution, and its optimal energy flows are presented. Optimizations are performed using the Cplex solver on an AMD A8-7200P Radeon R5, with a 2.4 GHz processing clock and 4 GB of RAM.

##### 4.1. Hourly greenhouse heat demand and solar collector heat production

The hourly heating demand of a one-hectare greenhouse, based on the weather condition of the case study region in 2019, is shown in Fig. 6. The total annual heating load is approximately 3 GWh. It can be seen that the heating demand has a significant seasonal effect, peaking at 1945 kW in winter and 249.7 kW in summer. In addition, the distribution of hours in different load ranges is illustrated in Fig. 7, which shows that the heating load exceeds 100 kW during 38.4 % of the hours of the year. The specific solar collector heat production is shown in Fig. 8. The maximum hourly specific collector output is 780.9  $\frac{W}{m^2}$ . The heat output of solar collector frequently equals zero during winter due to the lower temperature and solar irradiance.

##### 4.2. Minimum-cost solution

In this section, the developed tool is applied to determine the minimum-cost solution by considering two approaches: joint design-operation optimization and design optimization. Operation cost includes natural gas consumption and maintenance costs. As illustrated in Fig. 9, in the design optimization approach, a 1606.3 kW boiler almost satisfies the entire heating demand due to the lower cost of boiler than solar collector. While considering the joint design-operation approach, optimal supply capacities are converted to a 1264.5 kW boiler and a 1065.3 m<sup>2</sup> solar collector. Additionally, long-term heat storage capacity rises from 6.3 MWh to 25.1 MWh. Obtained results indicate that considering operation in addition to design reduces CO<sub>2</sub> emissions and total annual cost by 22.4 % and 6.6 %, respectively. This demonstrates the significance of joint design-operation optimization. Therefore, the base scenario in this research is the minimum-cost solution due to the joint design-operation approach, which is shifted to evaluate the effects of several scenarios in subsequent sections.

##### 4.3. Sensitivity analysis on the greenhouse set-point temperature

To demonstrate the validity of the model, a sensitivity analysis is

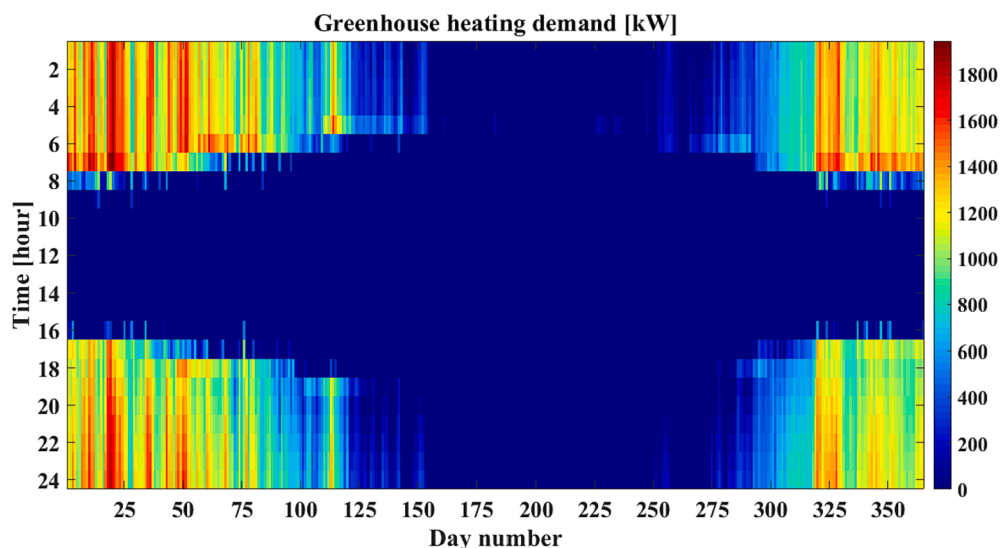


Fig. 6. Hourly heating load of greenhouse for the case study region in 2019.

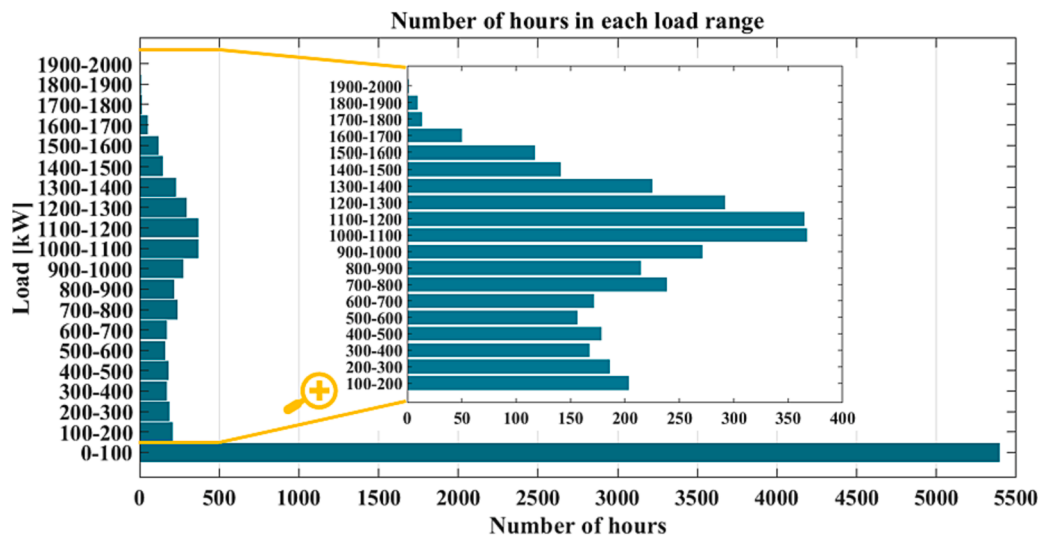


Fig. 7. Heating load distribution of greenhouse for the case study region in 2019.

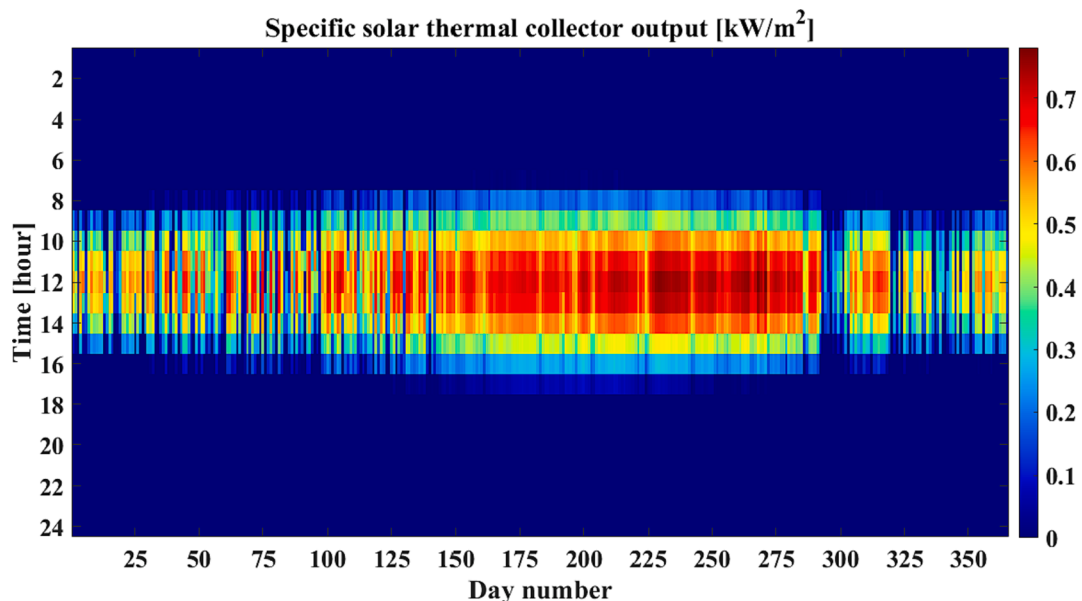


Fig. 8. Hourly specific solar collector heat production for the case study region in 2019.

conducted in this section by varying the greenhouse set-point temperature (heating load). As previously stated, the total heating demand in the base case ( $19^{\circ}\text{C}$  during the day and  $16^{\circ}\text{C}$  at night) is 3 GWh, and the relevant optimal energy system is outlined in section 4.2. As depicted in Fig. 10, as the greenhouse set-point temperature is raised, the required solar collector area increases significantly while boiler capacity increases gradually. In particular, an increase of  $1^{\circ}\text{C}$  in the greenhouse set-point temperature results in a rise of 8.6 % in heating demand, while the optimal solar collector area and boiler capacity increase by 25.1 % and 1.9 %, respectively. Moreover, it raises annual expenses by 7.3 % and  $\text{CO}_2$  emissions by 4 %.

#### 4.4. Impact of implementation of emission reduction policies

According to [58], the case study region will be severely affected by energy production and  $\text{CO}_2$  emissions by 2025, emphasizing the need for immediate emission reductions. This section evaluates the impact of emission reduction on the optimal energy system. The amount of emissions is restricted by applying constraints characterized by 30 %

and 50 % reductions compared to the conventional use of boilers for greenhouse heating. Following this, the results of the two reduction scenarios and the minimum-cost scenario are compared.

As shown in Fig. 11, 30 % and 50 % mitigations in  $\text{CO}_2$  emissions result in a 70.5 % and 220.5 % increase in solar collector area, as well as 9.9 % and 27.8 % boiler capacity reduction relative to the base minimum-cost solution, respectively. This occurs due to decreased natural gas consumption. The optimal solution for the 50 %  $\text{CO}_2$  reduction scenario contains a  $3414.7\text{-m}^2$  solar collector area in combination with 25 MWh long-term and 3.3 MWh short-term heat storage systems.

#### 4.5. Impact of reducing greenhouse cultivation period

As shown in Fig. 6, most of the heating load occurs during winter (December to March). The greenhouse cultivation schedule can affect the optimal energy system due to the required heating load. This effect is analyzed by comparing the year-round and two reduced cultivation period scenarios. Initially, the greenhouse heating demand is calculated considering the cultivation periods presented in Table 3 based on [59].

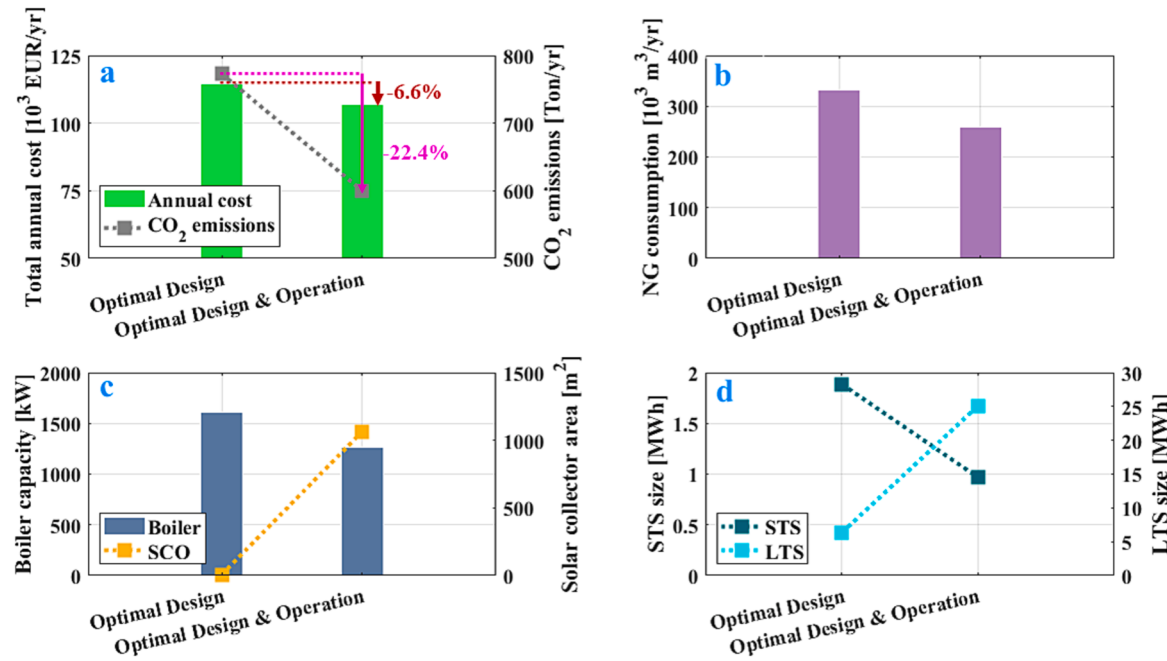


**Fig. 9.** Comparison of optimal characteristics of the investigated energy system considering minimum-cost solutions in joint design-operation optimization and design optimization approaches, including a) Total annual cost and CO<sub>2</sub> emissions, b) Decision variable: natural gas consumption, c) Decision variables: boiler capacity and solar collector (SCO) area, d) Decision variables: long-term heat storage (LTS) and short-term heat storage (STS) sizes.

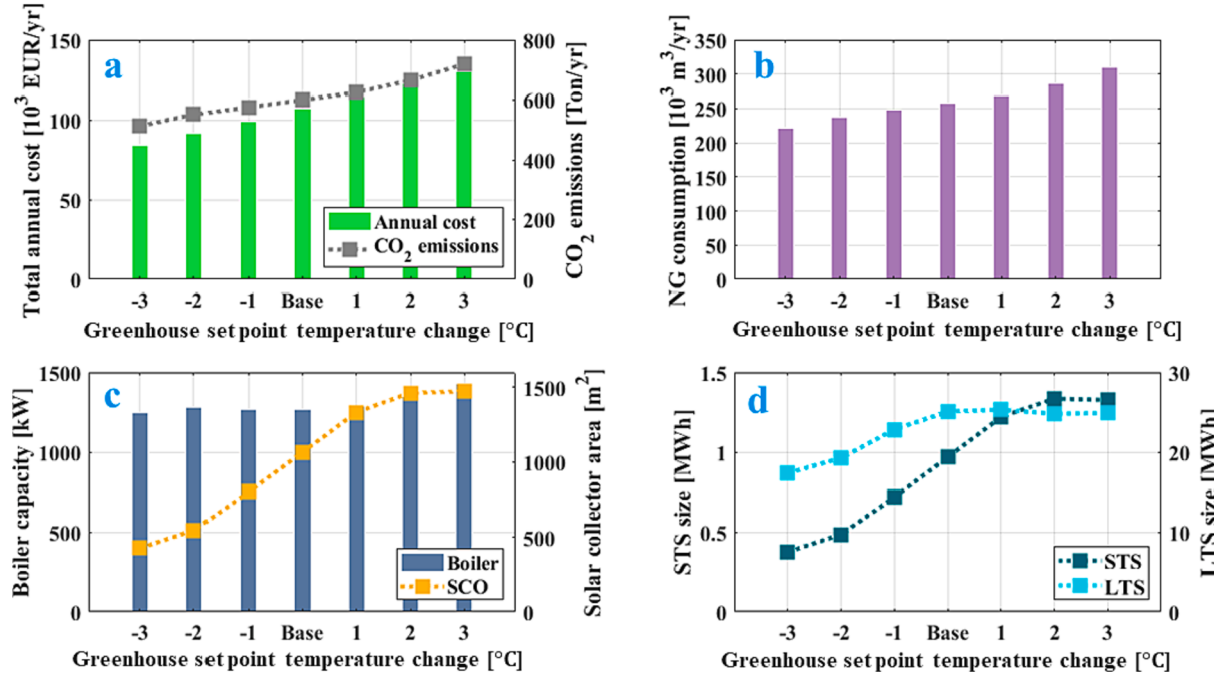


**Fig. 10.** Sensitivity analysis on heating load by varying greenhouse set-point temperature including a) Total annual cost and CO<sub>2</sub> emissions, b) Decision variable: natural gas consumption, c) Decision variables: boiler capacity and solar collector (SCO) area, d) Decision variables: long-term heat storage (LTS) and short-term heat storage (STS) sizes.

Then, the annual cost is minimized by taking the calculated heating demand into account. Finally, optimal outputs for year-round and reduced cultivation period scenarios are compared.

Under the first and second cultivation period scenarios, the total heating load of the greenhouse is reduced by about 36.1 % and 56.5 %, respectively. As shown in Fig. 12, the first reduced cultivation period decreases total annual cost by 32.4 % and CO<sub>2</sub> emissions by 28.3 %. In addition, the second reduced cultivation period decreases annual cost by

52.2 % while lowering emissions by 51.3 % compared to the year-round scenario. Therefore, by decreasing the cultivation season, both annual cost and CO<sub>2</sub> emissions are significantly reduced. Meanwhile, vegetable market demand is typically highest during the winter months.

#### 4.6. Impact of natural gas price and solar collector investment cost

The impact of natural gas price and solar collector investment cost

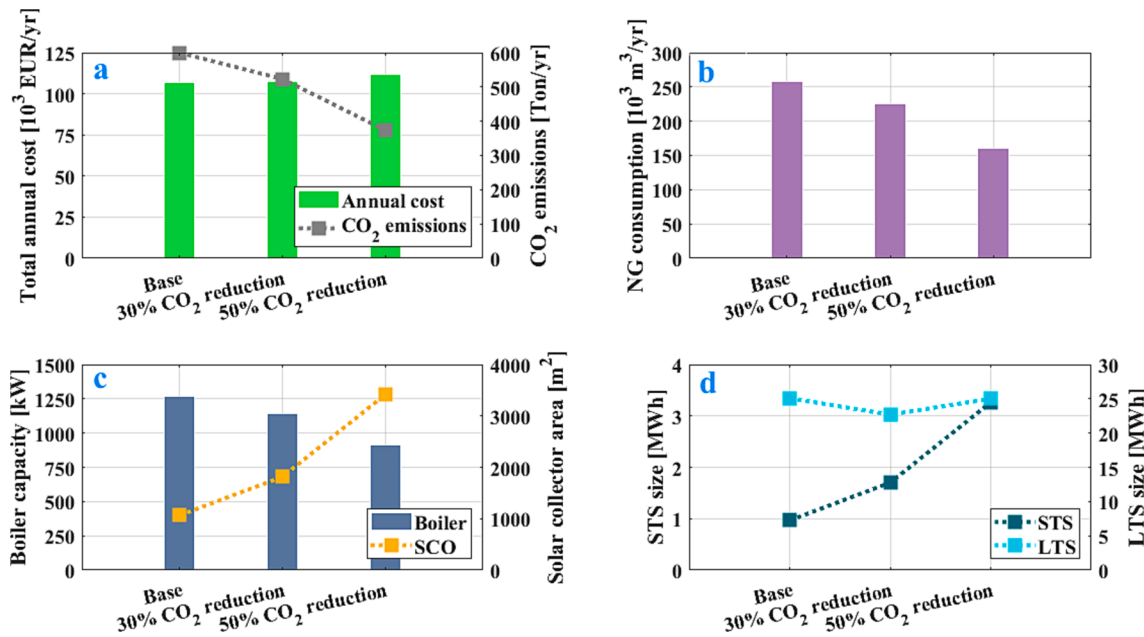


**Fig. 11.** Comparison of optimal characteristics of the investigated energy system considering different levels of CO<sub>2</sub> reduction, including a) Total annual cost and CO<sub>2</sub> emissions, b) Decision variable: natural gas consumption, c) Decision variables: boiler capacity and solar collector (SCO) area, d) Decision variables: long-term heat storage (LTS) and short-term heat storage (STS) sizes.

**Table 3**

Different cultivation period scenarios for tomato.

Cultivation scenario	Jan	Feb	Mar	Apr	May	Jun	Jul	Aug	Sep	Oct	Nov	Dec	Total demand [MWh/yr]	Peak demand [kW]
Year-round	X	X	X	X	X	X	X	X	X	X	X	X	3023	1945
Schedule 1	X	X	X	X	X	X	X	X	X	X	X	X	1930.8	1945
Schedule 2	X	X	X	X	X	X	X	X	X	X	X	X	1315.1	1745.2

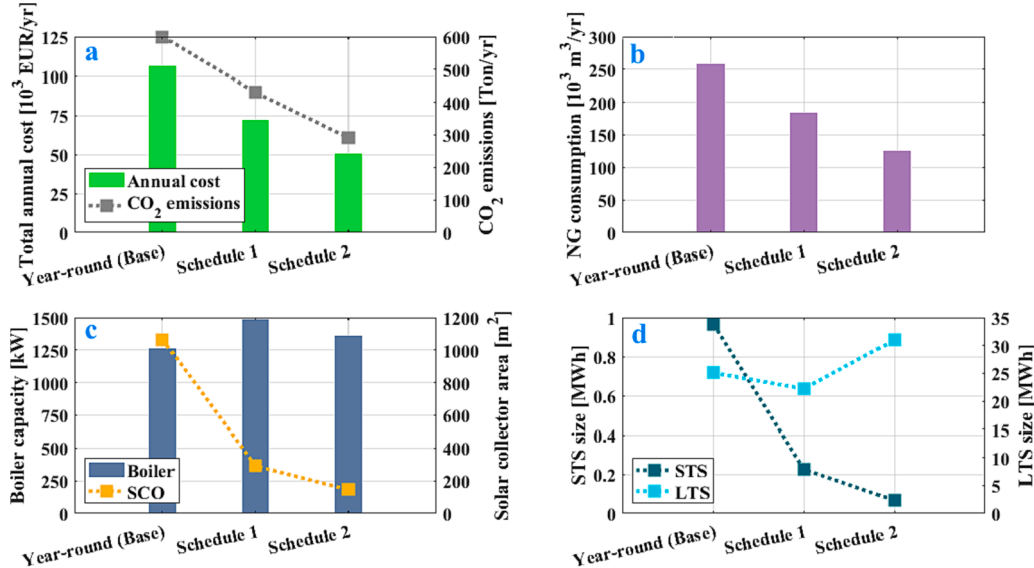


**Fig. 12.** Comparison of optimal characteristics of the investigated energy system considering the effect of cultivation scheduling, including a) Total annual cost and CO<sub>2</sub> emissions, b) Decision variable: natural gas consumption, c) Decision variables: boiler capacity and solar collector (SCO) area, d) Decision variables: long-term heat storage (LTS) and short-term heat storage (STS) sizes.

projections on optimal energy system capacities, annual cost, and CO<sub>2</sub> emissions are investigated in this section. Fig. 13 and Fig. 14 demonstrate that solar energy is not only used in environmentally friendly scenarios that mitigate carbon emissions but also transitioning to solar

energy is economically feasible in scenarios of rising natural gas price and decreasing solar collector investment cost.

As shown in Fig. 13, three different natural gas prices are taken into account because of the crucial effect of natural gas price on optimization

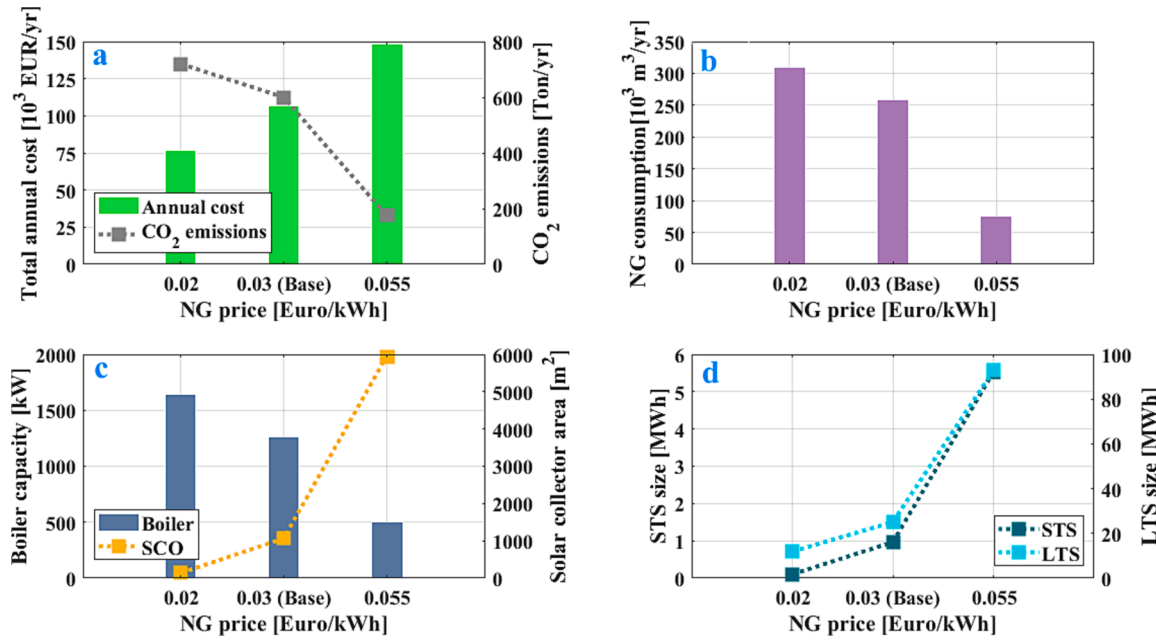


**Fig. 13.** Comparison of optimal characteristics of the investigated energy system considering different natural gas prices, including a) Total annual cost and  $\text{CO}_2$  emissions, b) Decision variable: natural gas consumption, c) Decision variables: boiler capacity and solar collector (SCO) area, d) Decision variables: long-term heat storage (LTS) and short-term heat storage (STS) sizes.

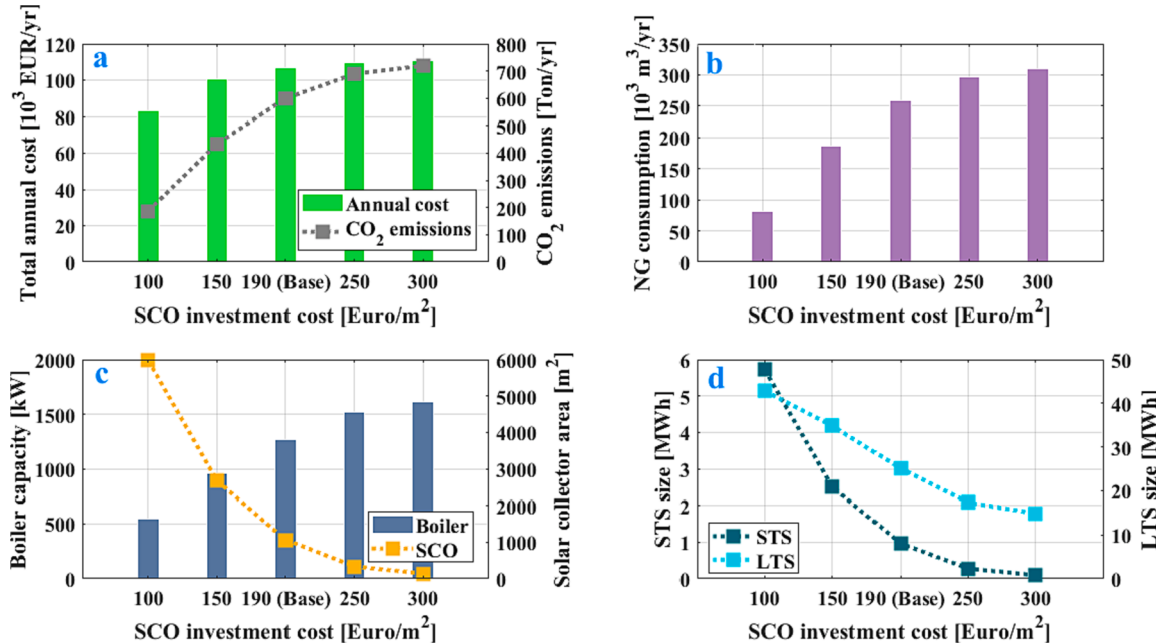


**Fig. 14.** Comparison of optimal characteristics of the investigated energy system considering different solar collector investment costs, including a) Total annual cost and  $\text{CO}_2$  emissions, b) Decision variable: natural gas consumption, c) Decision variables: boiler capacity and solar collector (SCO) area, d) Decision variables: long-term heat storage (LTS) and short-term heat storage (STS) sizes.

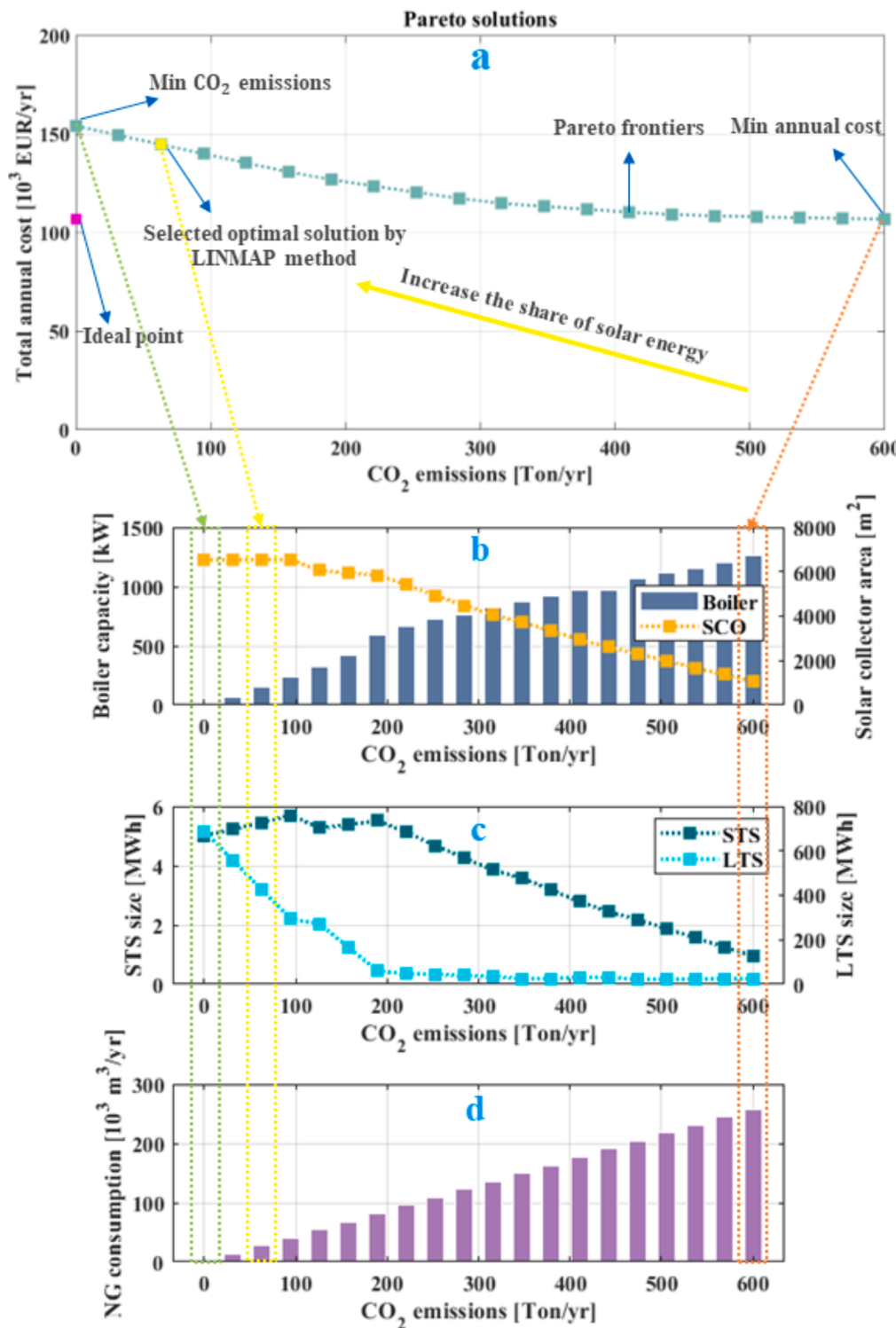
results, including export natural gas prices to Iraq and Turkey, as well as the EU-average natural gas price, equal to 0.02 [55], 0.03 [55] and 0.055 [54]  $\text{EUR}/\text{kWh}$ . According to Fig. 14, as the price of natural gas rises, the optimal solar collector area increases, and boiler size decreases. Consideration of 0.055  $\text{EUR}/\text{kWh}$  for natural gas price results in an increase of 38.7 % in annual cost and a decrease of 70.8 % in  $\text{CO}_2$  emissions compared to the base minimum-cost solution (0.03  $\text{EUR}/\text{kWh}$ ).

Fig. 14 illustrates the effect of solar collector investment cost on the optimal energy system. Five investment costs for solar collector are

considered: 300 [29], 250 [38], 190 [54], 150, and 100 (to assess the effect of lower costs)  $\text{EUR}/\text{m}^2$ . The solar energy share increases as solar collector cost decreases, particularly when costs are less than 190  $\text{EUR}/\text{m}^2$ . Comparing 100  $\text{EUR}/\text{m}^2$  to the base scenario (190  $\text{EUR}/\text{m}^2$ ), results in 22.5 % and 68.7 % reductions in annual cost and  $\text{CO}_2$  emissions, respectively.

#### 4.7. Multi-objective optimization

The trade-offs between two conflicting objectives of minimizing total



**Fig. 15.** The characteristics of Pareto optimal solutions, including a) Total annual cost and  $\text{CO}_2$  emissions, b) Decision variables: boiler capacity and solar collector (SCO) area, c) Decision variables: long-term heat storage (LTS) and short-term heat storage (STS) sizes, d) Decision variable: natural gas consumption.

annual cost and  $\text{CO}_2$  emissions are presented as Pareto frontiers. The supply capacities, heat storage sizes, and natural gas consumption of each optimal solution of the Pareto are shown in Fig. 15. The bi-objective optimization is performed by implementing the epsilon constraint method; therefore, reducing the maximum threshold of  $\text{CO}_2$  emissions increases the total annual cost and share of solar energy. Considering the minimum- $\text{CO}_2$  solution, the demand is entirely covered by solar energy. On the right side of the diagram, where the annual cost

objective dominates, the characteristics of the minimum-cost solution are presented with the highest amount of  $\text{CO}_2$  emissions.

After identifying Pareto optimal points, the LINMAP method is applied to rank these solutions regarding the relative closeness to the ideal solution (where both objectives are minimized). The selected optimal solution is also shown in Fig. 15, marked with a yellow square, which achieves 63.1 tonnes of  $\text{CO}_2$  emissions. Long-term heat storage reaches a peak SOC of 423.7 MWh in the selected solution. Moreover,

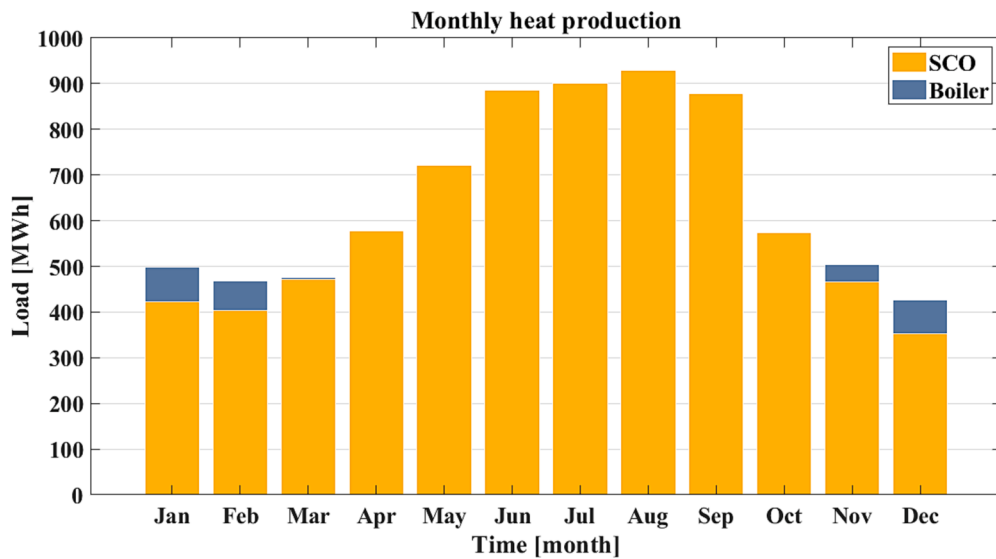


Fig. 16. Accumulated monthly heat production of solar collector (SCO) and boiler considering the selected optimal solution by LINMAP method.

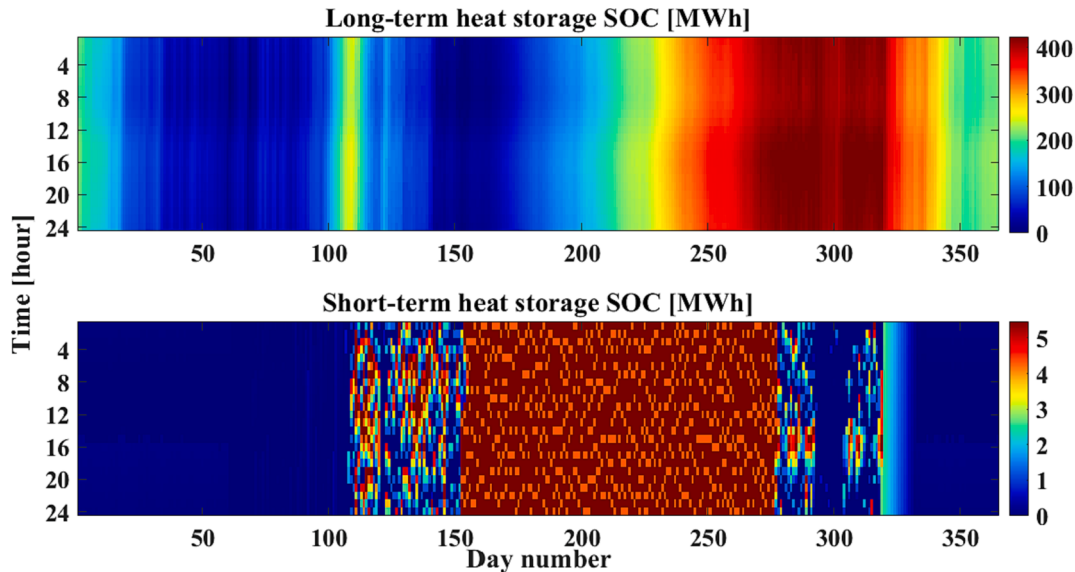


Fig. 17. Short-term and long-term heat storages state of charge considering the selected optimal solution by LINMAP method.

this solution combines a  $6540.4 \text{ m}^2$  solar thermal collector area with a 5.5 MWh short-term heat storage and a 155.8 kW boiler.

Fig. 16 expresses the optimal monthly heat production of the solar collector and boiler, considering the selected optimal solution. Solar collectors are the primary source of heat production, while boilers are used to provide additional heating during the winter months. The hourly state of charge of short-term and long-term heat storage systems is shown in Fig. 17. As can be seen, short-term heat storage serves as a buffer, while long-term storage has an apparent seasonal pattern. The long-term storage SOC is nearly zero at the end of May. Solar collectors gradually charge long-term storage during the spring and summer until the maximum SOC is reached in September; after that, it is depleted to meet the heat load, and the cycle repeats.

Table 4 indicates the solar collector area and heat storage sizes reported in previous greenhouse heating system studies. Low and high-temperature long-term thermal energy storage systems are simulated using TRNSYS software in [8]. Xu et al. [24] and Kim et al. [26] evaluated the thermal performance of a solar heating system with underground seasonal energy storage for greenhouse applications. However,

the reported values are affected by the location, greenhouse area, greenhouse set-point temperature, different techno-economic parameters, and different solar fractions.

In the following, the optimal collector area and solar fraction in our work are compared with those reported in similar studies. In Semple et al. [8], the ratio of solar collector area to greenhouse area is reported to be in the range of 21.5–50.2 %, and solar energy is responsible for 41–70 % of greenhouse total heating demand. The greenhouse location is in Ontario, Canada with an average temperature of  $-0.65^\circ\text{C}$  [43]. In another research in a different climate with an average temperature of  $17.1^\circ\text{C}$  [24], the ratio of solar collector area to greenhouse area is reported to be 21.7 % while the solar energy covers the heating demand completely in the entire year (100 % solar fraction).

Our optimization framework suggests the optimal ratio of solar collector area to greenhouse area to be in the range of 10.6–65.4 % (single and multi-objective functions) with a solar fraction of 33.3–96.7 %. The average temperature in this case study region is  $12.8^\circ\text{C}$  [43].

These analyses and comparisons demonstrate that our optimization

**Table 4**

Comparison of optimization results with prior papers.

Study	Methodology	Greenhouse Location/ Area	Solar collector area	Short-term storage capacity <sup>1</sup>	Long-term storage capacity <sup>2</sup>	Solar fraction <sup>5</sup>
[8]	Simulation (TRNSYS)	Ontario (Canada) / 4000 m <sup>2</sup>	861 m <sup>2</sup>	11.67 MWh	438.75 MWh	41 %
[24]	Evaluation of performance	Shanghai (China) / 2304 m <sup>2</sup>	2009 m <sup>2</sup>	11.67 MWh	630 MWh	70 %
[26]	Evaluation of performance	Yeoju (South Korea) / 3429 m <sup>2</sup>	(462 m <sup>2</sup> SCO)(234 m <sup>2</sup> PVT)	1.17 MWh	111.82 MWh	100 %
Current study	Optimization (Minimum-Cost)	Tehran / 10,000 m <sup>2</sup>	1065 m <sup>2</sup>	0.97 MWh	25.1 MWh	33.3 %
Current study	Bi-objective optimization	Tehran / 10000 m <sup>2</sup>	6540.4 m <sup>2</sup>	5.5 MWh	423.7 MWh	96.7 %

<sup>1</sup> Capacity of short-term heat storages in prior studies is calculated considering the volume reported in the article and also assuming  $\rho C = 4200 \frac{KJ}{m^3 \cdot K}$ ,  $\Delta T = 50 K$  according to [28].

<sup>2</sup> Capacity of long-term heat storages in prior studies is calculated considering the volume reported in the article and also assuming Energy density =  $22.5 \frac{KWh}{m^3}$  for

Borehole type (BTES) and Energy density =  $70 \frac{KWh}{m^3}$  for tank type (TTES) according to [60].

<sup>3</sup> BTES refers to borehole thermal energy storage.

<sup>4</sup> TTES refers to tank thermal energy storage.

<sup>5</sup> To compute the solar fraction of the current study, short-term heat storage is assumed as a greenhouse component.

results are within the range of similar studies and could be applied to further investigations considering different climatic conditions and objective functions.

## 5. Conclusion and future work

This research proposes an optimization framework for the joint design and hourly operation of a greenhouse-heating solar energy system. The hybrid energy system includes solar collectors, long-term and short-term heat storages, and a backup boiler. The minimum-cost solution is reached using Cplex solver. Afterward, optimal results are achieved by considering carbon reduction policies, greenhouse cultivation scheduling, natural gas pricing, and solar collector investment cost scenarios. Finally, using the epsilon-constraint method, multi-objective optimization is performed with the minimization of CO<sub>2</sub> emissions and annual cost as objectives. LINMAP determines the closest optimal solution of the Pareto front to the ideal point and its optimal size and energy flows. In summary, this study found:

- The joint design-operation optimization (decision variables: sizes of solar collector, natural gas boiler, and storage system in addition to heat flows) reduces CO<sub>2</sub> emissions by 22.4 % and the total annual cost by 6.6 %, compared to the design optimization approach (decision variables: sizes of solar collector, natural gas boiler and storage system). This shows the importance of considering operation decision variables in addition to sizing decision variables.
- The base minimum-cost solution (due to the joint design-operation approach) results in 599.9 tonnes of CO<sub>2</sub> emissions yearly. The optimal energy system consists of a 1264.5 kW boiler and a 1065.3 m<sup>2</sup> solar collector in combination with 967 kWh and 25.1 MWh short-term and long-term heat storages, respectively. In short, if the solar collector with an area of 10 % of the greenhouse area is utilized, the fossil fuel input to the greenhouse decreases by 19.7 % compared to the conventional use of boilers. More trade-offs could be discussed regarding land availability or fossil fuel limitations using our proposed optimization framework.
- The sensitivity analysis shows that implementation of decarbonization policy, such as considering 30 % and 50 % carbon emission reduction constraints, compared to the conventional use of boilers for heating greenhouses, causes a 70.5 % and 220.5 % rise in solar

collector area, as well as 9.9 % and 27.8 % boiler capacity reduction compared to the base minimum-cost solution, respectively.

- The reduced cultivation season (from January 1st to October 15th) decreases greenhouse heating load by 36.1 % compared to year-round agriculture. This cultivation schedule lowers annual cost by 32.4 % and CO<sub>2</sub> emissions by 28.3 %. However, the vegetable market demand in the period of October-January is generally the highest.
- The selected optimal solution of the Pareto front, which is the closest solution to the ideal point, has 35.3 % more annual cost and 89.5 % less CO<sub>2</sub> emissions than the minimum-cost solution. 5.5 MWh short-term and 423.7 MWh long-term heat storages, 155.8 kW boiler, and 6540.4 m<sup>2</sup> solar thermal collector area comprise this optimal energy system.

The developed framework in this paper can be implemented in future works to investigate how weather condition uncertainties affect the optimal results in real-world situations using stochastic optimization. Furthermore, it is beneficial to integrate electricity consumption of greenhouse, as well as the heating demand. It would also be valuable to consider more efficient heat storage systems with less land footprint, such as phase change materials or thermo-chemical heat storages.

## CRediT authorship contribution statement

**Parastoo Mohebi:** Conceptualization, Methodology, Software, Writing – original draft, Validation, Visualization. **Ramin Roshandel:** Supervision, Conceptualization, Methodology, Writing – review & editing.

## Declaration of Competing Interest

The authors declare that they have no known competing financial interests or personal relationships that could have appeared to influence the work reported in this paper.

## Data availability

Data will be made available on request.

## References

- [1] United Nations General Assembly, Transforming Our World: the 2030 Agenda for Sustainable Development, 2015, p. 1–5. <https://doi.org/1.1007/s10098-015-1076-9>.
- [2] Irabien A, Darton RC. Energy–water–food nexus in the Spanish greenhouse tomato production. *Clean Technol Environ Policy* 2016;18:1307–16. <https://doi.org/10.1007/s10098-015-1076-9>.
- [3] de Amorim WS, Valduga IB, Ribeiro JMP, Williamson VG, Krauser GE, Magtoto MK, et al. The nexus between water, energy, and food in the context of the global risks: An analysis of the interactions between food, water, and energy security. *Environ Impact Assess Rev* 2018;72:1–11.
- [4] Esmaili H, Roshandel R. Optimal design for solar greenhouses based on climate conditions. *Renew Energy* 2020;145:1255–65. <https://doi.org/10.1016/j.renene.2019.06.090>.
- [5] Barbosa G, Gadelha F, Kublik N, Proctor A, Reichelm L, Weissinger E, et al. Comparison of land, water, and energy requirements of lettuce grown using hydroponic vs. conventional agricultural methods. *Int J Environ Res Public Health* 2015;12(6):6879–91.
- [6] Hassani RHE, Li M, Dong LW. Advanced applications of solar energy in agricultural greenhouses. *Renew Sustain Energy Rev* 2016;54:989–1001. <https://doi.org/10.1016/j.rser.2015.10.095>.
- [7] Costantino A, Comba L, Sicardi G, Bariani M, Fabrizio E. Energy performance and climate control in mechanically ventilated greenhouses : A dynamic modelling-based assessment and investigation. *Appl Energy* 2021;288:116583. <https://doi.org/10.1016/j.apenergy.2021.116583>.
- [8] Semple L, Carriveau R, Ting DSK. A techno-economic analysis of seasonal thermal energy storage for greenhouse applications. *Energy Build* 2017;154:175–87. <https://doi.org/10.1016/j.enbuild.2017.08.065>.
- [9] Esen H, Esen M, Yuksel T. Modelling of biogas, solar and a ground source heat pump greenhouse heating system by using ensemble learning. Austria: New Dev Mech Mech Eng WSEAS Press Vienna; 2015. p. 74–81.
- [10] Burg V, Golzar F, Bowman G, Hellweg S, Roshandel R. Symbiosis opportunities between food and energy system: The potential of manure-based biogas as heating source for greenhouse production. Symbiosis opportunities between food and energy system The potential of manure-based biogas as heating source for greenhouse production 2021;25(3):648–62.
- [11] Esen M, Yuksel T. Experimental evaluation of using various renewable energy sources for heating a greenhouse. *Energy Build* 2013;65:340–51. <https://doi.org/10.1016/j.enbuild.2013.06.018>.
- [12] van Beveren PJM, Bontsema J, van Straten G, van Henten EJ. Optimal utilization of a boiler, combined heat and power installation, and heat buffers in horticultural greenhouses. *Comput Electron Agric* 2019;162:1035–48. <https://doi.org/10.1016/j.compag.2019.05.040>.
- [13] Cabeza LF. Advances in Thermal Energy Storage Systems: Methods and Applications. *Adv Therm Energy Storage Syst Methods Appl* 2014;1:592. <https://doi.org/10.1016/C2013-0-16453-7>.
- [14] Forough AB, Roshandel R. Lifetime optimization framework for a hybrid renewable energy system based on receding horizon optimization. *Energy* 2018;150:617–30. <https://doi.org/10.1016/j.energy.2018.02.158>.
- [15] Bakirci K, Yuksel B. Experimental thermal performance of a solar source heat-pump system for residential heating in cold climate region. *Appl Therm Eng* 2011;31:1508–18. <https://doi.org/10.1016/j.applthermaleng.2011.01.039>.
- [16] Zhang L, Xu P, Mao J, Tang X, Li Z, Shi J. A low cost seasonal solar soil heat storage system for greenhouse heating: Design and pilot study. *Appl Energy* 2015;156:213–22. <https://doi.org/10.1016/j.apenergy.2015.07.036>.
- [17] Hesaraki A, Holmberg S, Haghigiat F. Seasonal thermal energy storage with heat pumps and low temperatures in building projects - A comparative review. *Renew Sustain Energy Rev* 2015;43:1199–213. <https://doi.org/10.1016/j.rser.2014.12.002>.
- [18] Esen M. Thermal performance of a solar-aided latent heat store used for space heating by heat pump. *Sol Energy* 2000;69:15–25. [https://doi.org/10.1016/S0038-092X\(00\)00015-3](https://doi.org/10.1016/S0038-092X(00)00015-3).
- [19] Yang T, Liu W, Kramer GJ, Sun Q. Seasonal thermal energy storage: A techno-economic literature review. *Renew Sustain Energy Rev* 2021;139:110732. <https://doi.org/10.1016/j.rser.2021.110732>.
- [20] Antoniadis CN, Martinopoulos G. Optimization of a building integrated solar thermal system with seasonal storage using TRNSYS. *Renew Energy* 2019;56:66. <https://doi.org/10.1016/j.renene.2018.03.074>.
- [21] Ermis K, Findik F. Thermal energy storage Sustain Eng Innov 2020;2:66–88. <https://doi.org/10.1016/B978-0-08-087872-0-00307-3>.
- [22] Esen M, Ayhan T. Development of a model compatible with solar assisted cylindrical energy storage tank and variation of stored energy with time for different phase change materials. *Energy Convers Manag* 1996;37:1775–85. [https://doi.org/10.1016/0196-8904\(96\)00035-0](https://doi.org/10.1016/0196-8904(96)00035-0).
- [23] Esen M, Durmus A, Durmus A. Geometric design of solar-aided latent heat store depending on various parameters and phase change materials. *Sol Energy* 1998;62:19–28. [https://doi.org/10.1016/S0038-092X\(97\)00104-7](https://doi.org/10.1016/S0038-092X(97)00104-7).
- [24] Xu J, Li Y, Wang RZ, Liu W. Performance investigation of a solar heating system with underground seasonal energy storage for greenhouse application. Performance investigation of a solar heating system with underground seasonal energy storage for greenhouse application 2014;67:63–73.
- [25] Ataei A, Hemmatbady H, Nobakht SY. Hybrid thermal seasonal storage and solar assisted geothermal heat pump systems for greenhouses. *Adv Energy Res* 2016;4:87–106. <https://doi.org/10.12989/eri.2016.4.1.087>.
- [26] Kim DW, Kim MH, Lee DW. Economic and Environmental Analysis of Solar Thermal and Seasonal Thermal Energy Storage Based on a Renewable Energy Conversion System for Greenhouses. *Energies* 2022;15. <https://doi.org/10.3390/en15186592>.
- [27] van der Heijde B, Vandermeulen A, Salenbien R, Helsen L. Representative days selection for district energy system optimisation: a solar district heating system with seasonal storage. *Appl Energy* 2019;248:79–94. <https://doi.org/10.1016/j.apenergy.2019.04.030>.
- [28] Renaldi R, Friedrich D. Multiple time grids in operational optimisation of energy systems with short- and long-term thermal energy storage. *Energy* 2017;133:784–95. <https://doi.org/10.1016/j.energy.2017.05.120>.
- [29] Dorotić H, Pukšec T, Duić N. Economical, environmental and exergetic multi-objective optimization of district heating systems on hourly level for a whole year. *Appl Energy* 2019;251:113394. <https://doi.org/10.1016/j.apenergy.2019.113394>.
- [30] Wang H, Yin W, Abdollahi E, Lahdelma R, Jiao W. Modelling and optimization of CHP based district heating system with renewable energy production and energy storage. *Appl Energy* 2015;159:401–21. <https://doi.org/10.1016/j.apenergy.2015.09.020>.
- [31] Di Somma M, Graditi G, Heydarian-Foroushani E, Shafie-khah M, Siano P. Stochastic optimal scheduling of distributed energy resources with renewables considering economic and environmental aspects. *Renew Energy* 2018;116:272–87. <https://doi.org/10.1016/j.renene.2017.09.074>.
- [32] Gabrielli P, Gazzani M, Martelli E, Mazzotti M. Optimal design of multi-energy systems with seasonal storage. *Appl Energy* 2018;219:408–24. <https://doi.org/10.1016/j.apenergy.2017.07.142>.
- [33] Morvaj B, Evans R, Carmeliet J. Optimising urban energy systems: Simultaneous system sizing, operation and district heating network layout. *Energy* 2016;116:619–36. <https://doi.org/10.1016/j.energy.2016.09.139>.
- [34] Carpaneto E, Lazzeroni P, Repetto M. Optimal integration of solar energy in a district heating network. *Renew Energy* 2015;75:714–21. <https://doi.org/10.1016/j.renene.2014.10.055>.
- [35] Tulus V, Abokersh MH, Cabeza LF, Vallès M, Jiménez L, Boer D. Economic and environmental potential for solar assisted central heating plants in the EU residential sector: Contribution to the 2030 climate and energy EU agenda. *Appl Energy* 2019;236:318–39. <https://doi.org/10.1016/j.apenergy.2018.11.094>.
- [36] Durão B, Joyce A, Mendes JF. Optimization of a seasonal storage solar system using Genetic Algorithms. *Sol Energy* 2014;101:160–6. <https://doi.org/10.1016/j.solener.2013.12.031>.
- [37] Hirvonen J, ur Rehman H, Sirén K. Techno-economic optimization and analysis of a high latitude solar district heating system with seasonal storage, considering different community sizes. *Sol Energy* 2018;162:472–88.
- [38] Kotzur L, Markewitz P, Robinius M, Stolten D. Time series aggregation for energy system design: Modeling seasonal storage. *Appl Energy* 2018;213:123–35. <https://doi.org/10.1016/j.apenergy.2018.01.023>.
- [39] Pavicević M, Novosel T, Pukšec T, Duić N. Hourly optimization and sizing of district heating systems considering building refurbishment – Case study for the city of Zagreb. *Energy* 2017;137:1264–76. <https://doi.org/10.1016/j.energy.2017.06.105>.
- [40] Shah SK, Aye L, Rismanchi B. Multi-objective optimisation of a seasonal solar thermal energy storage system for space heating in cold climate. *Appl Energy* 2020;268:115047. <https://doi.org/10.1016/j.apenergy.2020.115047>.
- [41] Behzadi Forough A, Roshandel R. Multi objective receding horizon optimization for optimal scheduling of hybrid renewable energy system. *Energy Build* 2017;150:583–97. <https://doi.org/10.1016/j.enbuild.2017.06.031>.
- [42] Di Somma M, Yan B, Bianco N, Graditi G, Luh PB, Mongibello L, et al. Operation optimization of a distributed energy system considering energy costs and exergy efficiency. *Energy Convers Manag* 2015;103:739–51.
- [43] <https://www.renewables.ninja/>. Renewable.ninja (Accessed 16 January 2023).
- [44] Chen J, Zhao J, Xu F, Hu H, Ai QingLin, Yang J. Modeling of Energy Demand in the Greenhouse Using PSO-GA Hybrid Algorithms. *Math Probl Eng* 2015;2015:1–6.
- [45] Golzar F, Heeren N, Hellweg S, Roshandel R. A novel integrated framework to evaluate greenhouse energy demand and crop yield production. *Renew Sustain Energy Rev* 2018;96:487–501. <https://doi.org/10.1016/j.rser.2018.06.046>.
- [46] Van Beveren PJM, Bontsema J, Van Straten G, Van Henten EJ. Minimal heating and cooling in a modern rose greenhouse. *Appl Energy* 2015;137:97–109. <https://doi.org/10.1016/j.apenergy.2014.09.083>.
- [47] Andrews R, Pearce JM, Andrews R, Environmental JMP, Assessment E, Waste G. Environmental and Economic Assessment of a Greenhouse Waste Heat Exchange To cite this version : HAL Id : hal-02120486 Environmental and Economic Assessment of a Greenhouse Waste Heat Exchange 2019.
- [48] Heating ASABE. Ventilating and Cooling Greenhouses 2008.
- [49] Arcon-Sunmark A, Solar S. Collector Factsheet Arcon-Sunmark HT-SolarBoost 2017;35(10):2–3.
- [50] Kubisiński K, Szablowski Ł. Dynamic model of solar heating plant with seasonal thermal energy storage. *Renew Energy* 2020;145:2025–33. <https://doi.org/10.1016/j.renene.2019.07.120>.
- [51] Steen D, Stadler M, Cardoso G, Grossböck M, DeForest N, Marnay C. Modeling of thermal storage systems in MILP distributed energy resource models. *Appl Energy* 2015;137:782–92. <https://doi.org/10.1016/j.apenergy.2014.07.036>.
- [52] Sameti M, Haghigiat F. Optimization of 4th generation distributed district heating system: Design and planning of combined heat and power. *Renew Energy* 2019;130:371–87. <https://doi.org/10.1016/j.renene.2018.06.068>.
- [53] Esen H, Inalli M, Esen M. Technoeconomic appraisal of a ground source heat pump system for a heating season in eastern Turkey. *Energy Convers Manag* 2006;47:1281–97. <https://doi.org/10.1016/j.enconman.2005.06.024>.
- [54] Dorotić H, Pukšec T, Schneider DR, Duić N. Evaluation of district heating with regard to individual systems – Importance of carbon and cost allocation in cogeneration units. *Energy* 2021;221:119905.

- [55] <Https://www.tinn.ir/fa/tiny/news-186301>. Iran export gas price (Accessed 16 January 2023).
- [56] Buoro D, Pinamonti P, Reini M. Optimization of a Distributed Cogeneration System with solar district heating. *Appl Energy* 2014;124:298–308. <https://doi.org/10.1016/j.apenergy.2014.02.062>.
- [57] Sayyaadi H, Mehrabipour R. Efficiency enhancement of a gas turbine cycle using an optimized tubular recuperative heat exchanger. *Energy* 2012;38:362–75. <https://doi.org/10.1016/j.energy.2011.11.048>.
- [58] Mirzaei M, Bekri M. Energy consumption and CO<sub>2</sub> emissions in Iran, 2025. *Environ Res* 2017;154:345–51. <https://doi.org/10.1016/j.envres.2017.01.023>.
- [59] Forschungsinstitut für biologischen Landbau. Bioland Beratung GmbH. Biologischer Anbau im Biolandbau von Tomaten: Kompetenzzentrum Ökolandbau Niedersachsen; 2005.
- [60] Dahash A, Ochs F, Janetti MB, Streicher W. Advances in seasonal thermal energy storage for solar district heating applications: A critical review on large-scale hot-water tank and pit thermal energy storage systems. *Appl Energy* 2019;239:296–315. <https://doi.org/10.1016/j.apenergy.2019.01.189>.